Catalysis Letters, Vol. 117, Nos. 1–2, August 2007 (© 2007)
DOI: 10.1007/s10562-007-9143-4

High activity Ni/MoS_2 catalysts obtained from alkylthiometalate mixtures for the hydrodesulfurization of dibenzothiophene

M. Poisot,[a] W. Bensch,[a,*] S. Fuentes,[b] C. Ornelas,[c] and G. Alonso[c]

[a]*Institut für Anorganische Chemie, University of Kiel, Olshausenstr. 40-60 24118 Kiel, Germany*
[b]*Centro de Ciencias de la Materia Condensada, UNAM, Ensenada, Baja California, C.P. 22860, México*
[c]*Centro de Investigación en Materiales Avanzados S. C., Chihuahua, Chih, C.P. 31109, México*

Received 10 April 2007; accepted 17 May 2007

An efficient method for improving the catalytic properties of unsupported Ni/MoS_2 catalysts is mixing thiometalate precursors applying the appropriate precursors and thermal conditions. High active catalysts for the hydrodesulfurization (HDS) of dibenzothiophene (DBT) are prepared by the controlled decomposition of physical mixtures of $Ni(diethylentriamine)_2MoS_4$ (NDTA-TM) and $[(Propyl)_4N)]_2MoS_4$ (TPA-TM). The catalysts with a higher content of NDTA-TM are very active with a high selectivity for the direct desulfurization pathway (DDS) due to the synergistic effect of nickel. In addition the presence of a large amount of carbon may produce single-slabs of nickel promoted carbon containing molybdenum sulfides. The activity enhancement is attributed to an increased number of NiMoS active sites originated by the chemical interaction between the precursors NDTA-TM and TPA-TM during the mixing procedure. Furthermore, the carbon content in the final products is related to the enhancement of the activity and the preference of the DDS pathway. The controlled decomposition of mixtures of NDTA-TM + TPA-TM yields catalysts which are about twofold more active than an industrial $NiMo/Al_2O_3$ catalyst. This improvement may be attributed to an intense interaction of the precursors during the synthesis causing a re-dispersion of nickel atoms from NDTA-TM over the surface of carbon containing molybdenum sulfide provided by the precursor TPA-TM, increasing the amount of active sites. The catalysts from mixtures of $(NH_4)_2MoS_4$ (A-TM) and NDTA-TM behave similarly to the pure precursors.

KEY WORDS: thiometalates; Ni/MoS_2 catalysts; HDS of DBT; $Ni(diethylenetriamine)_2MoS_4$; $(NH_4)_2MoS_4$; $(Propyl_4N)_2MoS_4$.

1. Introduction

As the supply of low sulfur crude decreases, refineries are processing crude with high sulfur content meanwhile environmental regulation is becoming more and more restrictive for the gas emissions from diesel vehicles (50 wt ppm-S in Europe and Japan in 2005 [1,2]). Consequently the necessity to develop efficient hydrodesulfurization (HDS) catalysts is evident. The catalysts of choice for HDS of crude oils for many decades have been cobalt and nickel promoted molybdenum sulfides [3,4]. Recently new technologies for the production of ultra low sulfur diesel (ULSD) have been used in commercial hydrotreaters reaching < 10 ppm sulfur content in the products [5–7]. The actual hydrotreatment (HDT) catalysts are generally based on Mo and W sulfides commonly supported on alumina, and promoted with Co and Ni. Different preparation methods are used to synthesize unsupported HDS catalysts, e.g., comaceration [8], homogeneous sulfide precipitation [9], and thiosalt decomposition [10]. The catalytic properties of MoS_2 obtained by these methods are reported to depend strongly on the reacting atmosphere as well as on the heating conditions [8–10]. In others words, the properties depend on the experimental conditions applied during decomposition of precursor thiosalts and large variations in specific surface areas from few to several tenth of square meters per gram have been reported [11–16] The use of thiometalate complexes as precursors for the synthesis of active Co(Ni)MoS phases has provided enabled activity of the catalysts [15,17–23]. Recently a totally novel unsupported Ni_xWMoS_2 catalyst (NEBULA) was developed and commercialized by Exxon-Mobil and Akzo Nobel which presents an exceptional high activity [24]. Results like this encouraged us to search for new preparation routes yielding finally high efficient HDS catalysts. In the present work several mixtures of precursors containing only molybdenum A-TM ($(NH_4)_2MoS_4$) or TPA-TM ($[(Propyl)_4N)]_2MoS_4$) and nickel-molybdenum $Ni(diethylentriamine)_2MoS_4$ (NDTA-TM) were used in order to create functional Ni/MoS_2 catalysts for HDS of dibenzothiophene (DBT).

2. Experimental

The precursor NDTA-TM was prepared by reacting $NiCl_2$ and A-TM (molar ratio1:1) in 3 mL diethylenetriamine (100%) (dien) under solvothermal conditions in

*To whom correspondence should be addressed.
E-mail: wbensch@ac.uni-kiel.de

1011-372X/07/0800–0043/0 © 2007 Springer Science+Business Media, LLC

a Teflon lined steel autoclave at 120 °C for 6 days. The orange-red powder was obtained in 70% yield. The powder was filtered and washed with ethanol. However, the amount of the products obtained under solvothermal conditions is not enough for the HDS test reactions and a simpler synthesis route was developed. 10 mL aqueous solution of $NiCl_2$ (3.5 mmol) was mixed with dien (100%, 7 mmol) forming a pink solution. A-TM (3.5 mmol) dissolved in the minimum amount of water was added to this solution and immediately the product precipitated with 100% yield.

The precursors A-TM and TPA-TM were synthesized with the same method reported previously [25]. The mixtures of the catalyst precursors were manually ground in an agate mortar according to the Ni/Ni + Mo ratios shown in tables 1 and 2. The mixtures were then decomposed under N_2 atmosphere in a rotating glass tube (300 rpm) adapted for a Gero SR oven with Eurotherm controller. The tube was loaded with 1–3.6 g per batch. The temperature program was selected to obtain a surface-porous material. The mixtures presented in table 1 were placed into a preheated oven (285 °C) and then heated up to 500 °C within 2 h. This temperature was hold for 10 min followed by cooling down to 400 °C within 1 h, holding this temperature for other 2 h. The mixtures listed in table 2 were placed into a less hot preheated oven (100 °C), then heated up to 325 °C within 1.5 h and holding it for 20 min. After cooling down to 250 °C within 0.5 h the reaction products were removed from the oven. The samples were cooled down to room temperature under N_2 flow (0.4 L/min) and stored in this atmosphere. (N_2, Air Liquide 5.0). Chemical elemental analyses were performed with a EURO Vector EA Combustion analyzer using zinc sample holders filled with 2–3 mg. The samples were heated up to 1000 °C under oxygen atmosphere and the gases were detected by a thermal-conductivity cell. Far Infrared spectra were collected on a Bruker IFS 66 instrument. The samples were prepared in polyethylene matrix. Mid Infrared spectra were recorded on an ATI Mattson Genesis instrument preparing the samples in a KBr matrix. FT-Raman spectroscopy experiments were performed by a Bruker RSA 106 instrument equipped with a Nd/YAG-Laser (1064 nm). X-ray powder diffraction patterns were recorded on a STOE-Stadi P diffractometer operating with Cu $K\alpha_1$ radiation and a position sensitive detector. A Philips ESEM XL 30 microscope equipped with an EDAX analyzer was used to perform morphological studies and semi-quantitative elemental analyses. Micrographs were taken at different areas of the samples applying several magnifications. For DTA-TG experiments the samples were placed in Al_2O_3 crucibles under a dynamic nitrogen atmosphere (flow rate: 75 mL/min, purity 5.0). The curves were measured up to 500 °C with 4 °C/min heating rate. The TG curves were corrected for buoyancy and current effects. Specific surface area (SSA) determination was performed with a QUANTACHROM AUTOSORB-1 model by nitrogen adsorption using the BET isotherm method. Samples were degassed under flowing argon at 200 °C for 2 h before nitrogen adsorption. Mean standard deviation for specific surface area measurements is about 2%. The pore size distribution was obtained from the desorption branch following the BJH method.

The HDS of DBT has been extensively studied as a model reaction for HDS of petroleum feedstock [3]. Laboratory studies have been performed in pressurized flow and batch reactors [15,19,20,26,27]. Using batch reactors, useful information such as rate constants and

Table 1
Initial rate constants and selectivity, specific surface areas and total pore volume of catalysts obtained from A-TM + NDTA-TM mixtures

Catalyst	Ni/Ni + Mo	k (1×10^{-7}) [mol s^{-1} g^{-1}]	HYD/DDS	Surface area (m^2/g)	Pore volume (cm^3/g)
A-TM	–	4.8	1.68	9	0.023
A-TM + NDTA-TM (1:1)	0.3	4.5	0.26	8	0.023
A-TM + NDTA-TM (1:2)	0.4	4.7	0.29	22	0.063
A-TM + NDTA-TM (1:3)	0.428	6.5	0.23	40	0.118
NDTA-TM	0.5	6.7	0.28	43	0.110

Table 2
Initial rate constants and selectivity, specific surface areas and total pore volume of catalysts obtained from NDTA-TM + TPA-TM mixtures

Catalyst	Ni/Ni + Mo	k (1×10^{-7}) [mol s^{-1} g^{-1}]	HYD/DDS	Surface area (m^2/g)	Pore volume (cm^3/g)
TPA-TM	–	4.7	2.04	46	0.017
C3Mo025	0.25	19	0.82	26	0.014
C3Mo035	0.35	18	0.73	142	0.075
C3Mo040	0.40	19	0.61	2	0.003
C3Mo045	0.45	16	0.60	27	0.016
C3Mo050	0.50	20	0.28	13	0.009

selectivity can be obtained by following the composition of the reaction mixture as a function of time. The reaction was carried out in a Parr 4522 high-pressure batch reactor of 1 L. About 1 g of the precursor and 150 mL of a freshly prepared solution of DBT in decaline (5% wt/wt) were placed in the reactor. The reactor was then purged and pressurized with H_2 to 3.37 MPa and heated up to 350 °C at 10 °C/min heating rate. After reaching the working temperature, the products were collected for chromatographic analysis every half an hour to determine conversion versus time dependence. A Perkin Elmer Auto-System XL gas chromatograph equipped with a 9 ft × 1/8 inch packed column OV17 3% was used to analyze the collected samples. The main products obtained by HDS reaction of DBT were biphenyl (BP), cyclohexylbenzene (CHB) and tetrahydrodibenzothiophene (THDBT). The concentration of bicyclohexyl (BCH) was found to be negligible for all experiments. Selectivity was calculated as the mol percentage of the given product in the reaction mixture. The BP was produced through the so-called direct DDS pathway, and CHB and THDBT through the hydrogenation pathway (HYD), both pathways are parallel [28]. The ratio between HYD and DDS can be estimated in terms of the experimental selectivity by means of the CHB, THDBT and BP concentrations. The selectivity (HYD/DDS) can be approximately calculated by

$$\mathrm{HYD/DDS} = [\mathrm{CHB}] + [\mathrm{THDBT}]/[\mathrm{BP}].$$

For each catalyst the rate constant was calculated from the DBT conversion as function of time assuming that the DBT conversion being a pseudo-zero order reaction [9], according to the equation:

$$X_{DBT} = (1 - \eta DBT\,/\eta DBT) = (k/\eta_{DBT,0})\ t$$

where (X_{DBT} is the fraction of the DBT conversion, η_{DBT} = moles of DBT, k = pseudo-zero order rate constant, t = time in seconds and ($k/\eta_{DBT,0}$) is the slope. The mean standard deviation for catalytic measurements is about 2.5%. The catalysts reported here required a distinct activation time in the reactor. Therefore, only the data after the activation period were used for the evaluation of the catalytic activities.

3. Results

3.1. Catalytic activity and selectivity

3.1.1. Catalysts from mixtures of A-TM and NDTA-TM

The change of the molar concentration of DBT with reaction time (h) for catalysts obtained from A-TM, NDTA-TM and mixtures of them is presented in figure 1. The catalyst derived from A-TM shows a decrease of the DBT concentration almost in a linear

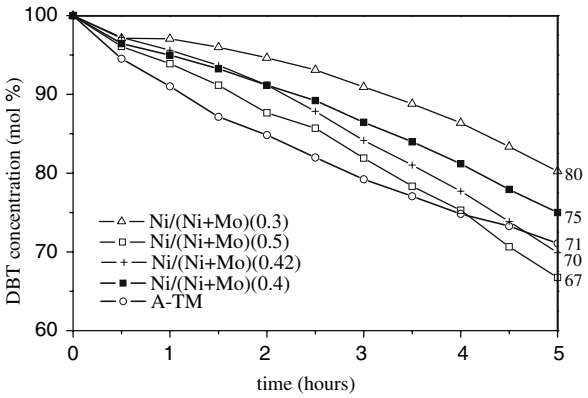

Figure 1. Time dependence of DBT conversion for catalysts obtained from A-TM + NDTA-TM mixtures and for a catalyst decomposing A-TM alone.

shape after an activation time, confirming that pseudo-zero order kinetics takes place under the experimental conditions used. The slight deviation from linearity observed at the end of the reaction is attributed to the deactivation of the catalyst by H_2S accumulated in the reactor. Hydrogen sulfide is known to have an inhibiting effect in the HDS reaction of DBT where the order depends on the partial pressure [29–31]. The formation of THDBT is favored at the beginning of the reaction but it declines at the end, showing a behavior like an intermediate compound [3], meanwhile CHB formation suits more a linear fit confirming the known trend of catalysts derived from A-TM for HYD (figure not shown). The catalytic activity (k, mol DBT/s g catalyst) was calculated using only the values from the second hour to the end of the reaction. The HYD/DDS ratio was measured after 5 h and the data are reported in table 1. The MoS_2 catalyst obtained from A-TM has a low activity ($k = 4.8 \times 10^{-7}$ mol/s g) and high selectivity for hydrogenation (HYD/DDS = 1.68). Catalysts derived from A-TM have been extensively studied and typically used as reference for unsupported catalysts in HDS tests [15,32,33]. The catalytic activity of Ni/MoS_2 catalysts obtained from NDTA-TM (figure 1) show a decrease of the DBT concentration during the reaction and again it can be assumed that the slope of the curve is linear after the activation time. The concentration of BP through the DDS pathway is largely favored for this catalyst starting from the beginning of the reaction (figure not shown). The catalysts obtained from its mixtures exhibit a very similar behavior producing also mainly BP. For all catalysts from mixtures of A-TM + NDTA-TM an increase of the slope with time is observed at the beginning of the experiment and no deactivation occurs at the end. The initial effect is assigned to a slow process of catalyst activation requiring H_2S generated from the reaction. The catalysts reach then their activated form after 2 h of reaction and remained very active up to end of the experiment without deactivation. The latter observation suggests that

the H_2S concentration during the last hour of the experiment is relatively low. In contrast to the low activity of the MoS_2 catalyst obtained from A-TM the Ni/MoS_2 material derived by the decomposition of NDTA-TM shows a high activity ($k = 6.7 \times 10^{-7}$ mol/s g) and a high selectivity for direct desulfurization (HYD/DDS = 0.28). A gradual increase of the activity of the catalysts is found with increasing nickel content (table 1). The activity of a commercial catalyst ($NiMo/Al_2O_3$) was characterized under the actual experimental conditions for comparison ($k = 12 \times 10^{-7}$ mol/s g, HYD/DDS = 0.53). The present catalysts prepared by decomposition of A-TM or NDTA-TM or mixtures of them exhibit lower constant rate values. But the materials derived by decomposition of A-TM and NDTA-TM mixtures are more selective for DDS than the commercial catalyst and the samples received from A-TM or NDTA-TM (table 1). The surface area of mixture catalysts measured after the catalytic test increases gradually with the amount of precursor NDTA-TM in the reaction mixture (table 1). A similar trend is observed for the pore volumes of the catalysts (table 1).

3.1.2. *Catalysts from mixtures of NDTA-TM and TPA-TM*

Figure 2 displays the change of the molar concentration of DBT as function of the reaction time for catalysts derived from precursor TPA-TM and mixtures of TPA-TM with NDTA-TM. The numerical results for k (mol DBT/s g catalyst) were calculated using the data after 2.5 h until the reaction end and the HYD/DDS ratios are compiled in table 2. The experiments were run for 6 h to compensate the time consumed at the beginning for the activation of the catalysts.

The catalytic activity pattern of MoS_2 obtained from TPA-TM is similar to that of the material received using A-TM as precursor with a linear decrease of DBT supporting the assumption of pseudo-zero order kinetics for the reaction. This catalyst has a similar activity (4.7×10^{-7} mol/s g) but a higher HYD/DDS selectivity

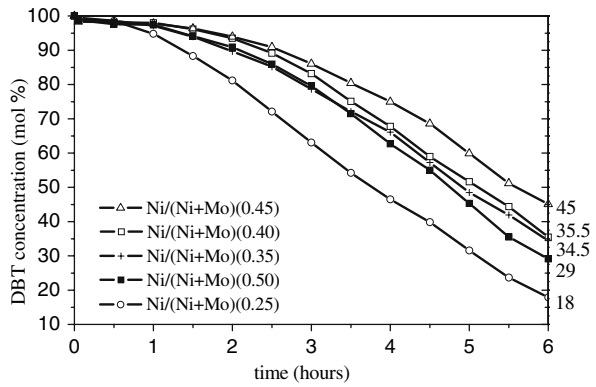

Figure 2. Time dependence of the DBT changes for catalysts obtained from NDTA-TM + TPA-TM mixtures.

(2.04) compared to the catalyst prepared by thermal decomposition of the precursor A-TM. Such a change of selectivity can be attributed to carbon introduced into the catalyst by the alkyl group of the TPA-TM precursor. It has been reported in literature that carbon influences both the activity and the selectivity in the HDS reaction of DBT [34–36]. All NDTA-TM + TPA-TM catalysts display an increase of the slope with reaction time at the beginning of the test, similarly to the results of A-TM + NDTA-TM catalysts. This behavior is attributed to a slow activation process requiring H_2S generated during the reaction. But materials processed by the decomposition mixtures of NDTA-TM + TPA-TM present more conversion of DBT after 6 h than catalysts of A-TM + NDTA-TM mixtures indicating that they contain more active sites for HDS. All catalysts produce increasing amounts of BP and CHB, while the concentration of THDBT reaches a maximum and decreases again (figure not shown). An interesting observation are the higher activities ($16–20 \times 10^{-7}$ mol/s g) than those obtained from single precursors. Moreover, the catalytic activities are much higher than the activity of the industrial supported catalyst (see above). The observed HYD/DDS ratios (0.28–0.82) represent a higher selectivity for DDS compared to $Ni-Mo/Al_2O_3$, and intermediate selectivity compared to data observed for materials from precursors A-TM or TPA-TM and the promoted sample from the precursor NDTA-TM. All catalysts show mainly the formation of BP (DDS route). Because the selectivity is linked with the mode of DBT adsorption, the large amount of BP formed during the reaction indicates that the DBT adsorption on the active phase occurs with the DBT molecule standing up in a vertical geometry. Thus, for all catalysts the flat DBT adsorption through the adsorption of π-electrons of DBT molecules favoring the hydrogenation route of the HYD reaction of DBT appeared more difficult than the direct C–S bond cleavage. The surface areas of the catalysts derived by thermal decomposition of mixtures of NDTA-TM + TPA-TM measured after the catalytic test show values ranging from 46 m^2/g (TPA-TM) to the largest one of 142 m^2/g for C3Mo035. This last sample also presents the highest pore volume. The other catalysts have relatively poor surface areas ranging from 2 to 27 m^2/g (table 2). These results suggest the effect of carbon support combined with the synergistic effect of nickel being at the optimum in C3Mo035, as previously observed when tetrabutylammonium thiometalate is used as a precursor combined with a cobalt promoter [37].

The most active catalysts were obtained from NDTA-TM + TPA-TM mixtures after an activation period at the beginning of the catalytic test. In order to study the chemical composition of the samples the analyses were performed before and after the catalytic test. Moreover, the samples obtained after the catalytic test were heated under inert atmosphere. These samples were then also

Table 3
Mass loss and chemical composition of catalysts obtained by decomposition of NDTA-TM + TPA-TM precursors after the thermal post-treatment to 500 °C

Catalyst	Mass loss (%)	Composition[a]
C3Mo025actTA	−11	$MoS_{2.2}Ni_{0.2}C_{0.7}$
C3Mo035actTA	−10.6	$MoS_{2.7}Ni_{0.7}C_{0.7}H_{0.5}$
C3Mo040actTA	−12.9	$MoS_{2.5}Ni_{0.6}C_{0.8}$
C3Mo045actTA	−10.6	$MoS_{2.8}Ni_{0.8}C_{0.7}$
C3Mo050actTA	−8.7	$MoS_{2.7}Ni_{1.3}C_{0.6}$

[a] Calculated from EDX and CHNS as combination of atom %.

analyzed carefully. Far-Infrared spectra, powder X-ray patterns and scanning electron micrographs were collected with the fresh materials and the catalysts after the HDS reaction of DBT.

3.2. Elemental analysis

The chemical compositions of the catalysts derived from mixtures of NDTA-TM + TPA-TM were calculated converting the chemical elemental data to atom percent and considering the atom percent ratio regarding molybdenum, nickel and sulfur obtained by semi-quantitative EDX analyses. In table 3 the compositions in the as prepared state and after the catalytic test (denoted with -*act*) are summarized. Due to the mixing procedure the Ni content of the as prepared samples increases whereas the carbon content significantly decreases and the sulfur content exhibits a moderate decrease. After the HDS reaction with DBT the composition of the catalysts show a remarkable increase of the sulfur content while the carbon content is further reduced. This tendency must be related to the activation time during the early stages of the test reaction. The two materials abbreviated as C3Mo035*act* and C3Mo050*act* in table 3 exhibit a good activity and selectivity. For both samples a similar trend of the chemical composition in comparison with the composition of the as prepared samples is observed, i.e., the sulfur content has increased about 2.6 times for the former and 3 times for the latter material. Simultaneously, the carbon content was reduced by 37.5% and 15%, respectively. The thermal post-treatment of the catalysts (see table 4) leads to a further decrease of the sulfur and carbon contents, with a much more pronounced reduction of the carbon content (41–62%) than for sulfur (about 15–32%). After the thermal post-treatment, the ratios of Mo:S and Mo:C are around 1:2.6 and 1:0.7, respectively, suggesting that after all these experiments the carbon content remaining in the materials could belong to the final stable catalyst structure.

3.3. Thermal analysis

After the HDS reaction with DBT the samples were studied by thermal analysis under an inert atmosphere up to 500 °C. Table 4 lists the mass changes determined with thermogravimetry experiments (samples are denoted with *actTA* at the end of the sample code). In general the decomposition occurs in a broad single step which is accompanied by a broad endothermic event. The decomposition starts at room temperature and is finished between about 400 °C and 430 °C. Most of the samples exhibit a mass loss of about 11%. But the catalysts with the highest Ni content shows the lowest mass loss while the sample with the lowest surface area has the highest mass loss, probably indicating that much more carbon particles cover the sample surface and not just support the structure. The sample C3Mo040 has the smallest pore volume of all mixtures and the highest carbon content after the catalytic test (see table 3) as well as after the thermal treatment (compare with table 4).

Table 4
Chemical compositions of catalysts obtained by the thermal decomposition of NDTA-TM + TPA-TM mixtures

Catalyst	C (wt %)	H	N	S	Ni/Mo[a]	S/Mo[a]	S	Mo	Ni	Composition[b]
							(wt %)			
C3Mo025	19	2.1	7.2	26.4	0.29	1.55	30.6	58.6	10.8	$MoS_{1.5}Ni_{0.2}C_3N_{0.9}H_4$
C3Mo035	20	2.3	8.9	26.3	0.3	1.18	25	63	12	$MoS_{1.2}Ni_{0.2}C_{2.4}N_{0.9}H_{3.3}$
C3Mo040	19.9	2.4	10.3	26.3	0.38	1.43	27.8	58.3	13.9	$MoS_{1.4}Ni_{0.3}C_{2.8}N_{1.2}H_{4.2}$
C3Mo045	16	1.7	8.9	27.2	0.58	1.42	25.7	54.5	19.8	$MoS_{1.4}Ni_{0.5}C_{2.2}NH_{2.8}$
C3Mo050	15.1	1.7	8.6	27.8	0.53	1.36	25.5	56.2	18.3	$MoS_{1.3}Ni_{0.9}C_{1.9}N_{0.9}H_{2.6}$
C3Mo025act	8.4	1.3	0.4	34.2	0.39	2.7	41.8	46.5	11.7	$MoS_{2.7}Ni_{03}C_{1.7}H_{3.3}$
C3Mo035act	6.7	1.3	0.5	32.2	0.75	3.14	41.5	39.9	18.6	$MoS_{3.2}Ni_{0.7}C_{1.5}H_{4.1}$
C3Mo040act	8.7	1.3	0.4	33.6	0.52	2.5	38.5	46.4	15.1	$MoS_{2.5}Ni_{0.5}C_{1.7}H_{3.1}$
C3Mo045act	6.5	0.9	0.5	34.3	0.93	2.51	34.9	41.4	23.7	$MoS_{2.5}Ni_{0.9}C_{1.2}H_{2.1}$
C3Mo050act	5.4	0.8	0.4	34.9	1.17	3.94	43.1	33.4	23.5	$MoS_{2.6}Ni_{1.4}CH_2$

[a] Calculated from EDX data as atom %.
[b] Calculated from EDX and CHNS as combination of atom %.
act = after the catalytic test.

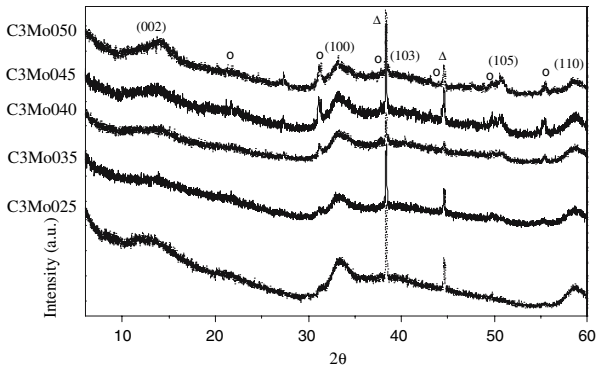

Figure 3. XRD patterns of TPA-TM + NDTA-TM mixtures after HDS of DBT. (hkl) = MoS_2 (JCPDS 371492), o = Ni_3S_2 (JCPDS 851802), Δ = Al (JCPDS 851327).

3.4. X-ray diffraction

Figure 3 shows the XRD patterns of the catalysts from mixtures of TPA-TM + NDTA-TM after the HDS reaction, while in figure 4 the patterns of the same catalysts after the thermal post-treatment are displayed. In both patterns the (002) reflection is observed as a broad and weak signal indicating that a poorly crystalline MoS_2 is obtained with a low layer stacking along the *c* direction. The overall features of the patterns are in agreement with those reported for poorly crystalline catalysts [37,38] and the shapes are also similar to those observed for a carbon-supported NiMo-sulfide prepared using active carbon and recorded after the catalytic test with DBT [39]. The similarity of the present X-ray powder patterns with that published previously [39] may be regarded as an indication for the formation of carbosulfide phases. Indeed this is not an evidence but can viewed as a hint for the occurrence of such phases. Weak and broad peaks of nickel sulfide are also detected. Note that the sharp reflections located at around 38.4 and 44.6° 2Θ are caused by the Al sample holder.

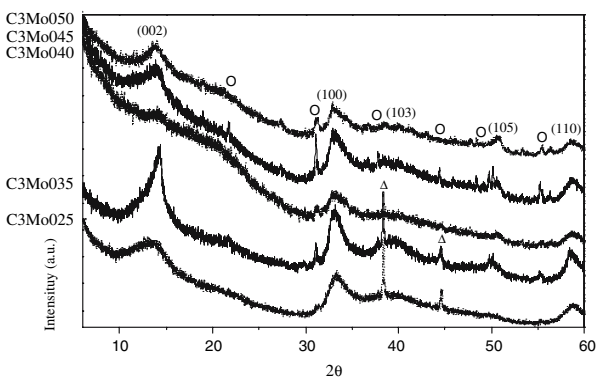

Figure 4. XRD patterns of NDTA-TM + TPA-TM mixtures after the HDS reaction and the thermal post-treatment to 500 °C. (hkl) = MoS_2 (JCPDS 371492), o = Ni_3S_2 (JCPDS 851802), Δ = Al (JCPDS 851327).

However, the C3Mo035 sample shows a rather homogeneous dispersion of nickel and the weakest (002) reflection of all catalysts. After the thermal post-treatment the powder pattern evidences a rather crystalline nature of the material (figure 4). The (002) peak is clearly more intense than for the other samples and the asymmetric shape on the low angle side may be due to the turbostratic disorder of the MoS_2 layers [40]. The reflections of Ni_3S_2 are still seen in the pattern. The pattern of C3Mo040*act* (after the catalytic test) indicates that the material is nearly amorphous against X-rays with a broad modulation at around 14° 2θ (see figure 3). Even after the post-treatment this sample seems to be the material with the lowest crystalline nature (compare figure 4).

3.5. IR spectroscopy

In table 5 the IR data of the catalysts before and after the thermal post-treatment are summarized. In general the absorption bands are broad and have a low intensity. For the Mo–S stretching modes two main bands are expected according to the layered nature of the MoS_2 crystallites, i.e., one band along the basal plane ($\perp$ *c*, 385 cm^{-1}) and another perpendicularly to the basal plane or along the c axis (// *c*, 467 cm^{-1}) [41]. In the IR spectra of all samples only a weak band around 383 cm^{-1} is registered. This band is asymmetric towards lower wave-numbers being attributed to strongly distorted monolayers of MoS_2 along the basal plane, as already detected by X-ray diffractometry. Moreover it is suggested that the pronounced asymmetry results from the partial incorporation of carbon into the MoS_2 structure, at least in the surface, and from increased bending and folding of the MoS_2 layers [34,45]. Recently, Raman studies of promoted catalysts obtained by urea-matrix combustion synthesis on alumina support revealed similar distortions of MoS_2 [46]. In the mid-IR region a broad band centered at around 1100 cm^{-1} is observed (see figure 5). This absorption

Table 5
IR data in cm^{-1} of catalysts obtained from NDTA-TM + TPA-TM mixtures

Sample	*v* Mo–S [41,42] ($\perp$ c)	*v* C_xS_n [43]	*v* Ni–Mo–C [44]
C3Mo025act	383	1127	1625
C3Mo035act	382	1082	1633
C3Mo040act	381	1120	1626
C3Mo045act	375	1119	1629
C3Mo050act	382	–	1628
C3Mo025actTA	383	1082	1635
C3Mo035actTA	383	1138	1636
C3Mo040actTA	383	–	1630
C3Mo045actTA	382	1092	1630
C3Mo050actTA	383	1093	1629

act = after catalytic test, actTA = thermal post-treatment after the catalytic test.

band was reported [47] to be accompanied by a weak signal at 830 cm^{-1} and is related to the intermediary products of the decomposition of dimethylsulfide forming polymeric $(C_xS)_n$ species [48]. May be in the present samples this band is caused by a carbosulfide phase at the edge-planes of MoS_2. Indeed, Berhault *et al*. have found that the interaction between carbon and sulfur not only favors the formation of surface carbosulfide phases, but also stabilizes texturally the sulfide particles that is reflected in improved catalytic stability and high catalytic performance [41,43].

The band at around 1630 cm^{-1} (see figure 5) may be the vibration of "Ni–Mo–C" entities resulting from the synergistic effect of nickel and carbon in molybdenum disulfide by the substitution of sulfur by carbon in an analogy of the synergistic effect of nickel and molybdenum carbide on alumina observed in IR spectra of adsorbed CO [1] or by pyridine adsorption on $NiMo_2C$/Al catalysts [44]. This band is not observed for the catalyst obtained from A-TM and remarkably the intensity of this absorption band increases with the nickel content in the TPA-TM + NDTA-TM catalyst mixtures. We note that for the most active catalyst (C3MoO35) this absorption band occurs at the highest frequency, even after the thermal post-treatment (see figure 5). The highest catalytic activity of the NiMoS based catalysts is a result of the synergistic effect. Whether the absorption band at around 1630 cm^{-1} is an indicator of the catalytic activity of a material must be investigated more in detail and research efforts are under way.

3.6. Scanning electron microscopy

The catalysts were characterized with scanning electron microscopy with a special focus onto the sample with the best catalytic activity, i.e., C3Mo035. In figure 6a–c the images of this material are shown before and after the catalytic test as well as after the thermal post-treatment, respectively. The as-prepared sample shows very fine surface porosity while after the catalytic test a wide variety of pore shapes ranging from very fine to very large pores

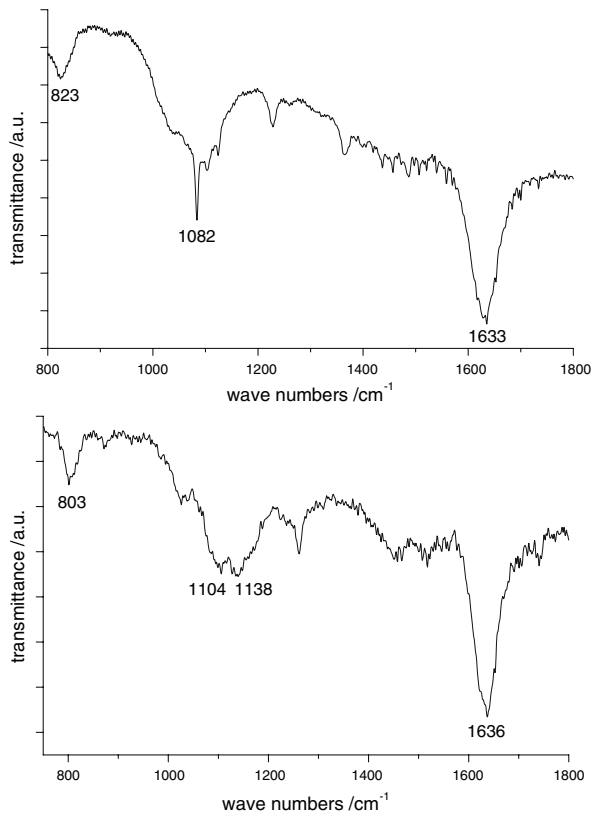

Figure 5. Infrared spectra of the catalyst C3MoO35 after the catalytic test (top) and after the thermal post-treatment (bottom). The wave numbers of the main vibrations are indicated.

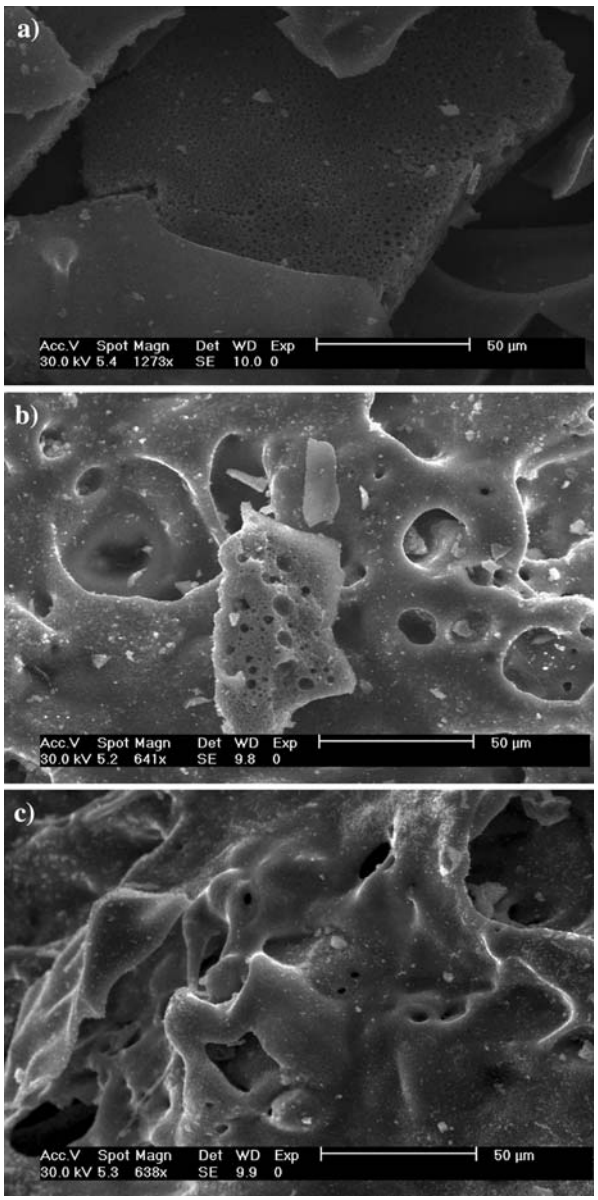

Figure 6. Scanning electron micrographs of the C3Mo035 catalyst, (a) fresh; (b) after HDS of DBT; (c) after the thermal post-treatment to 500 °C.

are seen and also distorted pores occur. The large range of pore sizes is related to the highest surface area measured for the catalyst series. After the thermal treatment the surface looks even more distorted containing some big pores. The other samples in this series have a significantly less pronounced surface porosity.

4. Discussion

The study of the effect of mixtures of different precursors onto the HDS activity was carried out following the principles of the method of *in situ* decomposition of thiosalts reported by Chianelli [19] and Alonso *et al.* [22,26,35]. Such a method comprises three important steps occurring in the reaction medium just before or at the beginning of the catalytic reaction: (a) Decomposition of the precursor; commonly thiomolybdates containing the MoS_4^{2-} ion like A-TM, which generates MoS_3 and then MoS_2 by successive fragmentation [10,49,50]; (b) Formation of MoS_2 nanoparticles resulting in a poorly-crystalline structure [38]; (c) Activation of MoS_2 by hydrogen/hydrogen sulfide gas mixtures in order to create S^{2-} vacancies, which are the active sites for HDS during the catalytic test [51]. In the present method the first and second steps are already completed by the thermal decomposition of the mixtures yielding fresh active catalysts.

However, the efficiency of the decomposition process to generate good catalysts depends on the type of the precursor and the chosen conditions [52]. The use of alkyl groups substituting the ammonium cation in A-TM has been shown to enhance the catalytic activity of MoS_2 catalysts [15,19,50]. Bithiometalates containing Co or Ni as precursors are also used to create very efficient HDS catalysts [53,54].

The catalysts derived from A-TM + NDTA-TM mixtures show a moderate activity enhancement up to the (Ni/Ni + Mo) ratio of 0.40. Then the well known synergistic effect of nickel originates a significant increase of the catalyst activity at the ratio of 0.428. The surface area and the pore volume also follow this tendency. The selectivity of catalysts obtained by the decomposition of A-TM is directed to HYD while the catalysts obtained from NDTA-TM and its mixtures prefer the DDS path evidencing the influence of nickel. These results are comparable to those reported in previous studies [22,35].

The catalysts derived from decomposition of NDTA-TM and TPA-TM show an important improvement of the activity by a factor of three compared with the catalyst generated only from NDTA-TM and almost twice the activity of a $NiMo/Al_2O_3$ industrial catalyst. This activity enhancement indicates that a chemical interaction between the precursors causes a better distribution of nickel in the mixtures obtained by NDTA-TM + TPA-TM, thus increasing the number of NiMoS active sites. The active sites for HDS reactions are recognized to be situated at the edges of MoS_2 crystallites forming NiMoS sites [55]. Recently, studies with scanning tunneling microscopy of the Co–Mo–S structure of HDS catalysts have shown that in single layer Co–Mo–S nanosheets the Co atoms are preferably located at the S-edge of MoS_2 [56]. Unfortunately, no infrared data were included in this report for comparison with our results. Nevertheless, the results of the different characterizations of the present catalysts highly suggest that the *in-situ* method produces catalysts consisting of very low stacking of Ni–Mo–S layers.

The Ni redistribution process among the NDTA-TM and TPA-TM precursors can take place through two ways, i.e., by the mixing of the precursors or by *in situ* decomposition of the precursors in the reaction media. The first pathway is controlled by the decomposition temperature while the second one is affected by the catalytic test conditions selected. The catalysts from mixtures of TPA-TM and NDTA-TM precursors were prepared at a relatively low final decomposition temperature yielding materials with modest surface porosity. X-ray diffraction experiments of these samples indicate that no crystalline nickel sulfides are formed. Infrared spectra show a vibration band around 1630 cm^{-1} which may be related to the Ni–Mo–C interactions, which is also observed in the fresh catalysts. Therefore, it is suggested that Ni was redistributed from the precursor NDTA-TM to TPA-TM during the mixing process, which can be viewed as an advantage of the modified *in situ* method. The *in situ* activation can also contribute to improve the activity that is obvious from figure 2. Most of the NDTA-TM + TPA-TM mixtures exhibit an increased slope of DBT conversion versus time after the first 1 or 2 h of reaction (activation time) indicating that more active sites are also formed during this time period. We note that for catalysts prepared from mixtures of A-TM + NDTA-TM an activation time is also required as can be seen in figure 1. A different behavior occurs for the catalyst derived from A-TM because much more DBT was converted in the first 1.5 h than during the rest of the reaction when the catalyst is activated. But after about 1.5 h the slope of the curve can be assumed to be linear. Besides the nickel redistribution in the catalysts obtained from TPA-TM + NDTA-TM mixtures a complementary effect may cause an enhancement of the activity when the optimum distribution of mesopores is reached. These mesopores are provided by the simultaneous decomposition of precursors NDTA-TM and TPA-TM generating an interconnected mesoporous network. In such optimized pore networks the DBT, BP and CHB molecules may diffuse more rapidly than in pores formed in single precursor catalysts. Confining effects that affect the selectivity of HDS of DBT have been suggested for mesoporous catalysts [11]. However,

more studies about the distribution of mesopores are needed in order to support this supposed model.

In the literature it was proposed that the degree of stacking of MoS_2 layers influences the activity/selectivity of unsupported catalysts [57]. Two different types of materials are distinguished [58]: supported type 1 catalysts which are not fully sulfided containing some Mo–O–Al linkages and supported type 2 catalysts being fully sulfided. According to this study type 1 phases are MoS_2 crystallites being in strong contact with the support material and type 2 catalysts can only be obtained by suppressing Mo-support interactions. Such type 2 materials can be achieved by using inert supports like carbon or complexing agents [58]. With respect to the relation between stacking of the MoS_2 slabs and catalytic activity of type 2 materials, highly active carbon supported MoS_2 catalysts with a very low stacking or even hardly any stacking have been reported [36,59]. It was stated that the active phase in MoS_2 based catalysts is present as few nanometers wide, single-layer, MoS_2-like nanoparticles which are promoted with Co or Ni. A profound STM study of the HDS activity of single-layer MoS_2 nanoclusters deposited on an Au substrate presented evidences for this assumption [60]. It was also demonstrated in the past that single-slab type 2 Co–Mo–S materials can be prepared [56]. The morphology of commercial Co/Ni promoted type 2 MoS_2 catalysts supported on γ-Al_2O_3 was recently studied applying X-ray diffraction, TEM and EDX experiments [61]. These catalysts were prepared by liquid-phase-sulfidation and several catalysts contained P as an additional additive. The main conclusions of the studies are: (i) such catalysts exhibit a high dispersion; (ii) a significant part of Ni segregates being present as separate Ni particles; (iii) MoS_2 stacking is not required for HDS of DBT; (iv) the sulfidation procedure significantly influences the morphology of type 2 catalysts, i.e., a treatment in H_2S/H_2 enhances the MoS_2 stacking whereas liquid-phase-sulfidation seems to prevent it; (v) MoS_2 stacking is not a prerequisite for a good performance and also not a sign of deactivation or lower activity. Studies of WS_2 supported on graphite performed by high-angle annular dark-field scanning transmission electron microscopy (HAADF-STEM) imaging revealed that single-slab structures will have the advantage of making more rim sites available for the reaction [62]. For multistack structures, only the top layer will expose the rim sites, increasing the rate of the DDS pathway [7].

The results of the investigations of the catalysts prepared by the controlled thermal decomposition of thiometalate precursors exhibit a preference for the DDS pathway during HDS of DBT. In view of the data of the chemical analyses, the results of the X-ray diffraction experiments, the catalytic performance and the state of knowledge in the literature the present catalysts are mainly low stacking MoS_2-like particles with Ni as promoter. The large amount of carbon may act as a support favoring the production of single-slab materials.

5. Conclusions

In the present study we demonstrated that the use of thiometalate mixtures in combination with the *in situ* activation method is a very promising method for the optimization of catalytic properties of Ni promoted, carbon containing molybdenum sulfide catalysts. These highly active catalysts are obtained by the controlled thermal decomposition of mixtures of the precursors A-TM, NDTA-TM, and TPA-TM.

The catalysts obtained from mixtures of the precursors NDTA-TM and TPA-TM exhibit an improved catalytic activity with a high selectivity for the DDS pathway due to the synergistic effect of nickel. The influence of the carbon content is clearly related with the enhancement of the activity and the preference of the DDS pathway, which both may be regarded as an evidence for the production of single-slab structure catalysts. The catalysts produced by controlled decomposition of NDTA-TM + TPA-TM are threefold and twofold more active than the catalyst produced by decomposition of the pure precursor NDTA-TM and the industrial $NiMo/Al_2O_3$ catalyst, respectively. Such an improvement is attributed to the interaction of the precursors during the mixing process that cause a re-dispersion of nickel atoms from precursor NDTA-TM over the surface of the carbon containing Mo sulfide provided by precursor TPA-TM, increasing the amount of active sites. The HYD/DDS selectivity ratio of the catalysts from NDTA-TM + TPA-TM mixtures is in-between of that of catalysts from the pure precursors NDTA-TM and TPA-TM. The catalysts derived from mixtures of A-TM and NDTA-TM show mainly an activity similar to the pure precursors.

Acknowledgments

The authors are grateful to E. Flores, F. Ruiz, G. Vilchez for technical assistance. S. Fuentes acknowledges grants from PAPIIT-UNAM IN119602-3 and CONACYT 41331-Y. Financial support by the German Science Foundation (DFG) is gratefully acknowledged by W. Bensch and M. Poisot (Project: DFG BE 1653/11-2).

References

[1] P. Da Costa, J.M. Manoli, C. Potvin and G.D. Mariadassou, Catal. Today 107 (2005) 520.
[2] N. Koizumi, Y. Urabe, K. Inamura, T. Itoh and M. Yamada, Catal. Today 106 (2005) 211.
[3] H. Topsøe, B.S. Clausen and F.E. Massoth, in: *Catalysis Science and Technology*, Vol. 11, eds. J.R. Anderson and M. Boudart (Springer, Berlin, 1996).
[4] R. Prins, V.H.J. De Beer and G.A. Somorjai, Catal. Rev. Sci. Eng. 31 (1989) 1.
[5] F.L. Plantenga, R. Cerfontain, S. Eijsbouts, F. van Houtert, G.H. Anderson, S. Miseo, S. Soled, K. Riley, K. Fujita and Y. Inoue, Stud. Surf. Sci. Catal. 145 (*Science and Technology in Catalysis*, 2002) (2003) 407.

[6] T. Fujikawa, H. Kimura, K. Kiriyama and K Hagirawa., Catal Today 111 (2006) 188.
[7] H. Topsøe, B. Hinnemann, J.K. Nørskov, J.V. Lauritsen, F. Besenbacher, P.L. Hansen, G. Hytoft, R.G. Egeberg and K.G. Knudsen, Catal. Today 107 (2005) 12.
[8] G. Hagenbach, Ph. Cosurty and B. Delmon, J. Catal. 31 (1973) 264.
[9] R. Candia, B.S. Clausen and H. Topsøe, J. Catal. 77 (1982) 564.
[10] M. Zdrazil, Catal. Today 3 (1988) 269.
[11] R. Frety, M. Breysse, M. Lacroix and M. Vrinat, Bull. Soc. Chim. Belg. 93 (1984) 663.
[12] K. Ramanathan and S.W. Weller, J. Catal. 95 (1985) 249.
[13] D.G. Kalthod and S.W. Weller, J. Catal. 95 (1985) 455.
[14] R.R. Chianelli, M. Daage and M. Ledoux, Adv. Catal. 40 (1994) 177.
[15] G. Alonso, M. Del Valle, J. Cruz-Reyes, V. Petranovskii, A. Licea-Claverie and S. Fuentes, Catal. Today 43 (1998) 117.
[16] F. Pedraza, S. Fuentes, M. Vrinat and M. Lacroix, Catal. Lett. 62 (1999) 121.
[17] G. Alonso, R.R. Chianelli and S. Fuentes, US Patent 2005/005945 A1.
[18] A.W. Naumann and A.S. Behan, US Patent 4,243,554 (1981).
[19] R.R. Chianelli and T.A. Pecoraro, US Patent 4,508,847 (1985).
[20] A.J. Jacobson, R.R. Chianelli and T.A. Pecoraro, US Patent 4,650,563 (1987).
[21] G. Alonso, V. Petranovskii, M. Del Valle, J. Cruz-Reyes, A. Licea-Claverie and S. Fuentes, Appl. Catal. A. 197 (2000) 87.
[22] G. Alonso, M.H. Siadati, G. Berhault, A. Aguilar, S. Fuentes and R.R. Chianelli, Appl. Catal. A. 263 (2004) 109.
[23] F. Pedraza and S. Fuentes, Catal. Lett. 65 (2000) 107.
[24] F.L. Plantenga and R.G. Leliveld, Appl. Catal. A. 248 (2003) 1.
[25] M. Poisot, W. Bensch, S. Fuentes and G. Alonso, Thermochim. Acta. 444 (2006) 35.
[26] G. Alonso, M. Del Valle, J. Cruz, A. Licea-Claverie, V. Petranovskii and S. Fuentes, Catal. Lett. 52 (1998) 55.
[27] D.J. Sajkowski and S.T. Oyama, Appl. Catal. A. 134 (1996) 339.
[28] D.D. Whitehurst, T. Isoda and I. Mochida, Adv. Catal. 42 (1998) 345.
[29] E. Olguin Orozco and M. Vrinat, Appl. Catal. A. 170 (1998) 195.
[30] H. Farag, I. Mochida and K. Sakanishi, Appl. Catal. A. 194 (2000) 147.
[31] B. Vogelaar, N. Kagami, A.D. van Langeveld, S. Eijsbouts and J.A. Moulijn, Prep. Pap.-Am. Chem. Soc., Div. Fuel Chem. 48 (2003) 548.
[32] M. Vrinat, M. Lacroix, M. Breysse and R. Frety, Bull. Soc. Chim. Belg. 93 (1984) 697.
[33] F. Zhang and P.T. Vasudevan, J. Catal. 157 (1995) 536.
[34] R.R. Chianelli and G. Berhault, Catal. Today 53 (1999) 357.
[35] G. Alonso, G. Berhault, A. Aguilar, V. Collins, C. Ornelas S. Fuentes and R.R. Chianelli, J. Catal. 208 (2002) 359.
[36] E.J.M. Hensen, P.J. Kooyman, Y. van der Meer, A.M. van der Kraan, V.H.J. de Beer, J.A.R. van Veen and R.A. van Santen, J. Catal. 199 (2001) 224.
[37] H. Nava, C. Ornelas, A. Aguilar, G. Berhault, S. Fuentes G. Alonso, Catal. Lett. 86 (2003) 257.
[38] K. Liang, R.R. Chianelli, F.Z. Chien and S.C. Moss, J. Non-Cryst. Solids 79 (1986) 251.
[39] M. Kouzu, Y. Kuriki, F. Hamdy, K. Sakanishi, Y. Sugimoto and I. Saito, Appl. Catal. A. 265 (2004) 61.
[40] D.L. Bish and J.E. Post (eds) *Modern Powder Diffraction in Reviews in Mineralogy*, Vol. 20 (Bookscrafters, Washington DC 1989).
[41] G. Berhault, A. Mehta, A.C. Pavel, J. Yang, L. Rendon, M.J. Yacaman, L. Cota Araiza, A.D. Moller and R.R. Chianelli, J. Catal. 198 (2001) 9.
[42] O. Monteiro and T. Trindade, Mater. Res. Bull. 39 (2004) 357.
[43] G. Berhault, L. Cota Araiza, A.D. Moller, A. Mehta and R.R. Chianelli, Catal. Lett. 78 (2002) 81.
[44] J.M. Manoli, P. Da Costa, M. Brun, M. Vrinat, F. Mauge and C. Potvin, J. Catal. 221 (2004) 365.
[45] R.R. Chianelli, G. Berhault, P. Santiago, D. Mendoza, A. Espinoza, J.A. Ascencio and M.J. Yacaman, Mater. Tech. 15 (2000) 54.
[46] S.L. Gonzalez-Cortes, S.M.A. Rodulfo-Baechler, T. Xiao and M.L. Green, Catal. Lett. 111 (2006) 1.
[47] C.H. Chang and S.S. Chan, J. Catal. 72 (1981) 139.
[48] B. Krebs and G. Gattow, Z. Anorg. Allg. Chem. 338 (1963) 225.
[49] E. Diemman and A. Müller, Coord. Chem. Rev. 10 (1973) 79.
[50] J. Brito, M. Ilija and P. Hernandez, Thermochim. Acta. 256 (1995) 325.
[51] P. Raybaud, J. Hafner, G. Kresse and H. Toulhoat, in: *Proc 2nd Int Symp on Hydrotreatment and Hydrocraking of oil fractions*, eds. B. Delmon, G.F. Froment and P. Grange (Elsevier, 1999) p. 309.
[52] J.V. Lauritsen, M.V. Bollinger, E. Lægsgaard, K.W. Jacobsen, J.K. Nørskov, B.S. Clausen, H. Topsøe and F. Besenbacher, J. Catal. 221 (2004) 510.
[53] W. Eltzner, M. Breysse, M. Lacroix and M. Vrinat, Polyhedron 5 (1986) 203.
[54] E.I. Stiefel, W.H. Pan, R.R. Chianelli and T.C. Ho, US pat. 4,581,125 (1986).
[55] H. Topsøe, B.S. Clausen, N.Y. Topsøe and P. Zeuthen, Stud. Surf. Sci. Catal. 53 (1989) 77.
[56] J.V. Lauritsen, S. Helveg, E. Lægsgaard, I. Stensgaard, B.S. Clausen, H. Topsøe and F. Besenbacher, J. Catal. 197 (2001) 1.
[57] M. Daage and R.R. Chianelli, J. Catal. 149 (1994) 414.
[58] E.J.M. Hensen, V.H.J. de Beer, J.A.R. van Veen and R.A. van Santen, Catal. Lett. 84 (2002) 59.
[59] P. da Silva, N. Marchal and S. Kasztelan, Stud. Surf. Sci. Catal. 106 (1997) 353.
[60] J.V. Lauritsen, M. Nyberg, J.K. Nørskov, B.S. Clausen, H. Topsøe, E. Lægsgaard and F. Besenbacher, J. Catal. 224 (2004) 94.
[61] S. Eijsbouts, L.C.A. van den Oetelaar and R.R. van Puijenbroek, J. Catal. 229 (2005) 352.
[62] A. Carlson, M. Brorson and H. Topsøe, J. Catal. 227 (2004) 530.